Virial Exchange–Correlation Energy Density in Hooke's Atom

KIN-CHUNG LAM, FEDERICO G. CRUZ, KIERON BURKE

Department of Chemistry, Rutgers University, 315 Penn Street, Camden, New Jersey 08102

Received 18 August 1997; revised 16 January 1998; accepted 16 February 1998

ABSTRACT: Application of the virial theorem to the interelectronic Coulomb repulsion shows that the virial of the exchange potential yields the exchange energy. However, the virial of the correlation potential does not yield the correlation energy. We have recently constructed a ''hypercorrelated'' potential whose virial *is* the correlation energy. We apply these ideas to a system which contains two interacting electrons in an external harmonic potential, Hooke's atom. This system can be solved analytically for a set of spring constants and numerically for any spring constant. By inverting the Kohn–Sham equations, the exact exchange and correlation potentials can be found. These exact values are compared with several popular approximate functionals, namely local spin density (LSD), Perdew, Burke, and Ernzerhof (PBE), and Becke and Lee–Yang–Parr (BLYP). We illustrate our results for two values of the spring constant. At a moderate value, the density is comparable to the He atom, while for a low spring constant, we explore extremely low densities. Int J Quant Chem 69: 533–540, 1998

Key words: density functional; exchange-correlation; energy density; Hooke's atom

Background

Kohn–Sham spin-density functional theory [1] is a formally exact orbital description of an interacting electronic system. The Kohn–Sham equations are, in atomic units ($e^2 = \hbar = m = 1$) for a spin-unpolarized system,

$$\{-\nabla^2/2 + v_S(\mathbf{r})\}\phi_i(\mathbf{r}) = \epsilon_i\phi_i(\mathbf{r}), \qquad (1)$$

where $\rho(\mathbf{r}) = \sum_{i=1}^{N}|\phi_i(\mathbf{r})|^2$ is the exact density, $v_S(\mathbf{r})$ is the Kohn–Sham potential, and the sum is over the lowest N-occupied orbitals. The total energy of the system is

$$\begin{aligned} E &= T_S + V_{\text{ext}} + U + E_{\text{XC}} \\ &= -\frac{1}{2}\sum_{i=1}^{N}\int d^3r\,\phi_i\,\nabla^2\phi_i + \int d\mathbf{r}\,\rho(\mathbf{r})v_{\text{ext}}(\mathbf{r}) \\ &\quad + \int d\mathbf{r}\int d\mathbf{r}'\,\frac{\rho(\mathbf{r})\rho(\mathbf{r}')}{2|\mathbf{r}-\mathbf{r}'|} + E_{\text{XC}}, \end{aligned} \qquad (2)$$

where T_S is the noninteracting kinetic energy, U is the Hartree energy, V_{ext} is the external potential energy, and E_{XC} is the exchange–correlation energy. The Kohn–Sham potential is found from knowing the density functional dependence of the

Correspondence to: K. Burke.

Contract grant sponsor: Research Corporation.

CCC 0020-7608 / 98 / 040533-08

contributions to the energy:

$$v_S(\mathbf{r}) = v_{\text{ext}}(\mathbf{r}) + \int d^3r' \frac{\rho(r')}{|\mathbf{r} - \mathbf{r}'|} + v_{\text{XC}}(\mathbf{r}), \quad (3)$$

where

$$v_{\text{XC}}(\mathbf{r}) = \frac{\delta E_{\text{XC}}[\,\rho]}{\delta \rho(\mathbf{r})}. \quad (4)$$

For practical calculations, only the exchange–correlation energy density functional $E_{\text{XC}}[\,\rho]$ needs to be approximated. Its exact definition comes from inverting Eq. (2):

$$E_{\text{XC}} = E - T_s - U - V_{\text{ext}}. \quad (5)$$

In Eq. (5), if the exact functional $E_{\text{XC}}[\,\rho]$ were available, we would have solved all N-electron problems, and many of us would be out of work. Fortunately, so far this exact functional form is not known, and so it is necessary to explore the form of this term, in order to make useful approximations.

Numerous functional approximations have been made to $E_{\text{XC}}[\,\rho]$. In the local spin density (LSD) approximation [1], the energy is written as:

$$E_{\text{XC}}^{\text{LSD}}[\,\rho] = \int d\mathbf{r}\, e_{\text{XC}}^{\text{unif}}(\,\rho(\mathbf{r})), \quad (6)$$

where $e_{\text{XC}}^{\text{unif}}(\,\rho)$ is the exchange–correlation energy density of a uniform gas of density ρ. While proving extremely reliable, LSD is insufficiently accurate for calculating bond energies, typically overbinding molecules [2]. In the last decade, more accurate generalized gradient approximations (GGAs),

$$E_{\text{XC}}^{\text{GGA}}[\,\rho] = \int d\mathbf{r}\, e_{\text{XC}}^{\text{GGA}}(\,\rho(\mathbf{r}), \nabla\rho(\mathbf{r})) \quad (7)$$

have made density functional theory popular in quantum chemistry. Now the approximation for the energy density uses not only the density at each point but also its gradient. Several popular forms exist for the function $e_{\text{XC}}^{\text{GGA}}(\,\rho, \nabla\rho)$, including a sequence of refinements developed by Perdew and co-workers [3–7]. More accurate still are hybrid schemes which mix some exact exchange with GGA exchange–correlation [8–10].

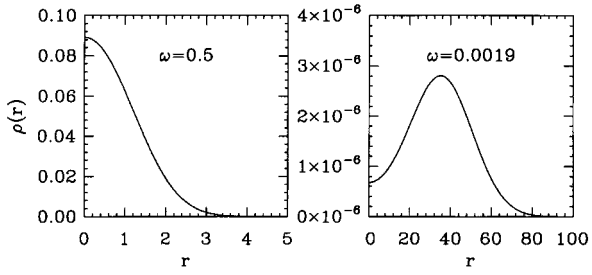

FIGURE 1. Density in Hooke's atom.

Hooke's Atom

To illustrate our results throughout this article, we consider the system of two electrons interacting via the Coulomb repulsion but in an harmonic potential. This system has recently received considerable attention in density functional theory, as both a pedagogical model and testing ground for various ideas. Kais et al. [11] pointed out that it could be solved analytically at a certain spring frequency ($\omega = \frac{1}{2}$), while Taut [12] showed that there existed an infinite discrete set of lower frequencies at which it could be solved analytically. We choose to study the Kais solution, which has a moderate density comparable to that of the He atom, as plotted on the left of Figure 1. A simple way to characterize the mean density is given by the average Seitz radius, defined in [13]. For the He atom, $\langle r_s \rangle = 1.6$, while for the Hooke's atom at $\omega = \frac{1}{2}$, $\langle r_s \rangle = 3.0$. Core electrons typically have $\langle r_s \rangle$ less than about 1, while valence electrons have $\langle r_s \rangle$ between about 1 and 6. The important qualitative differences from the He atom are the lack of a cusp at $r = 0$ (in fact, $\nabla\rho = 0$ here) and the Gaussian decay at large r.

For small ω, many aspects of this picture change because the densities involved are far lower than those encountered in most valence electron problems. We will look in particular at the case where the power series solution for the wave function truncates after the tenth power, for which $\omega \approx 0.0019$ [12], and $\langle r_s \rangle = 77$. Since this system was also studied by Filippi et al. [14], this will make comparison with previous calculations easier. As shown on the right of Figure 1, the density is no longer monotonically decreasing. It has a minimum at $r = 0$, rises to a maximum near $r = 35$, and then decays as a Gaussian. In the limit of extremely small ω, the density approaches a pure Gaussian centered at the classical (zero kinetic

energy) separation for the two electrons, at $r = (2\omega)^{-2/3}$ [12].

For a spin-unpolarized two-electron system, the single Kohn–Sham orbital $\phi(\mathbf{r})$ can be extracted directly from the electronic density:

$$\phi(\mathbf{r}) = [\tfrac{1}{2}\rho(\mathbf{r})]^{1/2}. \tag{8}$$

More generally, there now exist several methods in the literature [15–22] for constructing the Kohn–Sham potential and orbitals from a given density for any number of electrons. From the exact density, we can extract the exchange–correlation potential by inverting Eq. (3):

$$v_{\mathrm{XC}}(\mathbf{r}) = \epsilon_{\mathrm{KS}} + \frac{1}{2}\frac{\nabla^2\psi}{\psi} - \frac{1}{2}\omega^2 r^2 - \int \frac{\rho(\mathbf{r}')}{|\mathbf{r} - \mathbf{r}'|}\, d\mathbf{r}', \tag{9}$$

where ϵ_{KS} is the Kohn–Sham eigenvalue. In a spin-unpolarized two-electron system, the exact exchange potential v_x is given by minus one-half of the Hartree potential:

$$v_X(\mathbf{r}) = -\frac{1}{2}\int \frac{\rho(\mathbf{r}')}{|\mathbf{r} - \mathbf{r}'|}\, d\mathbf{r}', \tag{10}$$

and

$$E_X[\,\rho] = -\frac{1}{4}\iint \frac{\rho(\mathbf{r}')\rho(\mathbf{r})}{|\mathbf{r} - \mathbf{r}'|}\, d\mathbf{r}\, d\mathbf{r}', \tag{11}$$

so that

$$v_C(\mathbf{r}) = v_{\mathrm{XC}}(\mathbf{r}) - v_X(\mathbf{r}), \tag{12}$$

and $E_C = E_{\mathrm{XC}} - E_X$. The exact exchange potential can now be extracted from any density [23].

The exact values for the various energy components of interest here are listed in Table I. All of these have already appeared in earlier work [14]. Consider first the moderate density case. The correlation energy is of order one-tenth of the exchange energy, while the correlation-kinetic energy, T_C, is comparable to E_C, but of opposite sign. Thus $E_C + T_C$, which is negative [24], is much smaller in magnitude than E_C. This is typical of moderate density systems, in which the energy components' magnitudes are ordered by their leading powers in perturbation theory in powers of the interelectronic Coulomb repulsion. We have $E_X \sim O(e^2)$, $E_C \sim O(e^4)$, and $E_C + T_C \sim O(e^6)$, so that $|E_X| \gg |E_C| \gg |E_C + T_C|$. (In density functional theory, the appropriate perturbation theory is in powers of the coupling constant λ [25] along the adiabatic connection, as described later.) For the low-density case, however, E_C is a fifth of E_X, and T_C is noticeably less than $|E_C|$ because low-density correlation is dominated by the potential contribution.

We next consider the values of energy components within various functional approximations. The approximate functionals we use in our work are LSD, using the parametrization of Perdew and Wang [26], and two generalized gradient approximations, namely PBE and BLYP. Perdew, Burke, and Ernzerhof (PBE) [7] is the latest of the nonempirical Perdew functionals, which are derived from general exact conditions on the exchange–correlation hole, and the uniform and slowly varying electron gases. BLYP consists of Becke 88 [27] for exchange, and Lee–Yang–Parr correlation [28], both functionals which have been fit to the energies of specific finite systems. We also performed all calculations with PW91, finding very small energy differences with PBE, and very similar potentials, except that some oscillations in the PW91 potentials were removed in the PBE versions [7].

For the moderate density case, LSD as usual underestimates exchange by about 10% and overestimates correlation by about 100%, for both E_C and T_C. The GGAs both do much better for both exchange and correlation, with LYP being noticeably better than PBE for both E_C and T_C. For the

TABLE I
Energies for Hooke's atom (in millihartrees).

	$\omega = \frac{1}{2}$				$\omega = 0.0019$			
Component	Exact	LSD	PBE	BLYP	Exact	LSD	PBE	BLYP
E_X	−515	−441	−493	−502	−19.49	−17.38	−19.57	−20.08
E_C	−39	−86	−51	−35	−3.62	−10.84	−8.38	−3.20
T_C	29	47	36	26	1.95	2.04	1.84	0.11
$E_C + T_C$	−9	−39	−16	−9	−5.57	−8.80	−6.53	−3.09

low-density system, a similar picture arises for LSD, but PBE seriously overestimates $|E_C|$, although LYP is quite accurate. However, PBE gets T_C about right, while LYP seriously underestimates it.

Exchange–Correlation Potentials

Although density functionals are designed to reproduce total energies and energy differences, there has always been interest in examining other quantities, to gain further insight into the errors in the approximate functionals, with the hope of improving them [29]. In particular, many have studied the potentials which can be extracted from the models of the exchange–correlation energies via Eq. (4) and compared them with exact potentials, known for small systems from wave function calculations. Typically, there are very noticeable differences between the approximate functionals and the exact results. While the significance of these differences can be argued [30], the procedure for calculating the potentials is well-defined by Eq. (4), and the resulting curves definite.

In Figure 2, we plot the exact and several approximate exchange potential evaluated on the exact density. None of the functionals yield potentials which look like the exact exchange potential. The exact potential decays as $-1/r$ for large r (a universal feature), while both the LSD and all GGAs vanish exponentially. At small r, the exact potential goes to a constant quadratically with r. This qualitative behavior *is* reproduced by the approximate functionals. In contrast, in Coulombic atoms, divergences occur in the GGA potentials at the nucleus.

For the low-density case, no current approximate density functional should be expected to perform well. In fact, the GGAs look worse than LSD. At small r, neither LSD nor the exact exchange potential show much structure. For both B88 and PBE, the exchange potentials have significant structure for small r, where the density and its gradient change rapidly.

In Figure 3, we plot the exact and approximate correlation potentials. At large r, the exact correlation potential approaches 0 from above with a power law [14], while all the approximate functionals vanish rapidly, due to the Gaussian decay of the density. PBE and LYP decay particularly rapidly, due to the cutoff of correlation when the reduced density gradient becomes large. The slower decay of the LSD potential is closest to that of the exact. At small r, the approximate functionals are again qualitatively correct, but not quantitatively. No functional yields a positive value for the correlation potential at $r = 0$.

Exchange–Correlation Energy Densities

Similarly, there have been attempts in the past to compare the energy density with those of the functional approximations [31, 32]. Unfortunately, the energy density typically suffers from an ambiguity of definition, since the addition of *any* quantity which integrates to zero over the system does not alter the resulting energy. In particular, specification of a functional approximation does not uniquely specify an energy density. This problem is highlighted by the exchange GGAs of Perdew and co-workers, in whose derivation there is an integration by parts [33], which alters the energy density at each point.

A partial remedy to this difficulty is to choose a specific definition of the energy density, usually one that can be easily extracted from a wave function calculation. Again in the case of exchange, a common choice is an exchange energy density which comes from an integration over the ex-

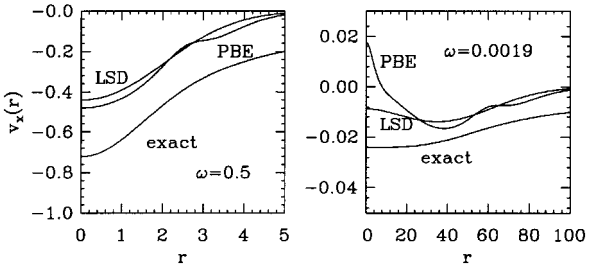

FIGURE 2. Exchange potential in Hooke's atom.

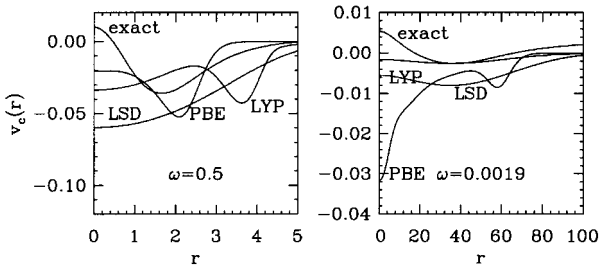

FIGURE 3. Correlation potential in Hooke's atom.

change hole:

$$e_X^{\text{hole}}(\mathbf{r}) = \rho(\mathbf{r}) \int d\mathbf{r}'\, \rho_X(\mathbf{r}, \mathbf{r}')/2|\mathbf{r} - \mathbf{r}'|, \quad (13)$$

where $\rho_X(\mathbf{r}, \mathbf{r}')$ is the exchange hole density surrounding an electron at $\mathbf{r}$. However, there is no way to calculate this quantity from the definitions of the approximate functionals. In particular, the energy densities given in Eqs. (6) and (7) are *not* necessarily approximations to the quantity defined in Eq. (13).

Virial Energy Densities

However, there is a choice of energy density which is *uniquely* determined by the functional. For example, in the case of exchange [34], the virial theorem yields [24]

$$E_X = -\int d\mathbf{r}\, \rho(\mathbf{r})\mathbf{r} \cdot \nabla v_X(\mathbf{r}). \quad (14)$$

Thus the definition

$$e_X(\mathbf{r}) = -\rho(\mathbf{r})\mathbf{r} \cdot \nabla v_X(\mathbf{r}) \quad (15)$$

provides a choice of energy density whose value is determined by the potential, and therefore directly by the functional itself.

For a spherical density, as is the case here, we may write

$$E_X = \int_0^\infty dr\, e_X^{\text{radial}}(r), \quad (16)$$

where

$$e_X^{\text{radial}}(r) = -\pi r^3 \rho(r) \frac{dv_X}{dr}. \quad (17)$$

Figure 4 is obtained from Figure 2 by differentiating the curve, and multiplying by $-4\pi r^3\rho(r)$. The area between this curve and the r-axis is then simply E_X.

An immediate conclusion from this figure is that although the various potentials look different, their corresponding exchange energy densities look similar. This is because the weighting factor in Eq. (17) is small both near $r = 0$ and at large r. Furthermore, in the middle, where the bulk of the contribution to the exchange energy occurs, the *slopes* of the various potentials are similar, even though the exact potential is significantly below

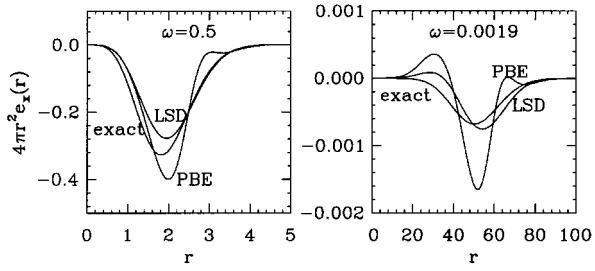

FIGURE 4. Radial virial exchange energy density in Hooke's atom.

the approximate ones. The LSD exchange energy density is almost everywhere noticeably below the exact energy density, reflecting the typical 10% underestimation of the magnitude of the exchange energy in LSD. LSD looks closer to the exact curve than the GGAs. However, the net area under the curve is more accurately given by the GGAs than by LSD, due to tremendous error cancellation. Similarity of potentials is not necessary for accurate energies.

In the case of correlation, the virial of the correlation potential yields [24]

$$-\int d\mathbf{r}\, \rho(\mathbf{r})\mathbf{r} \cdot \nabla v_C(\mathbf{r}) = E_C + T_C, \quad (18)$$

where T_C is the correlation contribution to the kinetic energy, i.e., the virial of the correlation potential *does not* yield the correlation energy. We define

$$e_C(\mathbf{r}) + t_C(\mathbf{r}) = -\rho(\mathbf{r})\mathbf{r} \cdot \nabla v_C(\mathbf{r}). \quad (19)$$

In Figure 5, the energy densities of Eq. (18) are constructed from Figure 3 by exactly the same procedure as for exchange. However, since $E_C + T_C$ is very small (it vanishes in the high-density limit), the net area between the r axis and the exact radial energy density curve is small. Consider first $\omega = \frac{1}{2}$.

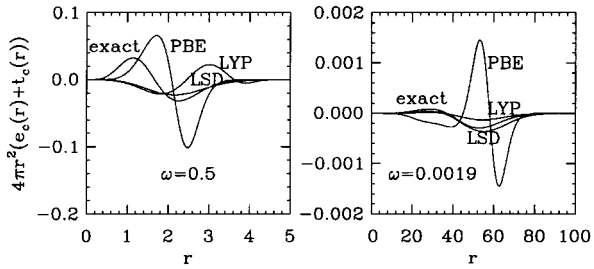

FIGURE 5. Radial virial correlation energy density in Hooke's atom.

There is a large cancellation between the positive peak near $r = 1$ and the negative peak near $r = 2$. This highlights a major deficiency of the LSD correlation potential. Because the density is monotonically decreasing, so too is the LSD correlation potential, so that its virial energy density is everywhere negative. Thus there is no cancellation between peaks, leading to an LSD prediction for this quantity which is a factor of 4 too negative. The GGA potentials, on the other hand, are not monotonic, allowing cancellations within the virial integral. The dip in the PBE correlation curve around $r = 2.2$ leads to an energy density similar to the exact one, but with too strong peaks. The two extrema at r about 2.5 and 3.5 in the LYP potential produce an energy density curve which may appear upside-down relative to the exact one, but whose net area is highly accurate.

Turning next to the lower density system, we see that the LSD curve again looks best, and this remains true for the energy densities. Interestingly, there is now a strong difference between LYP and PBE, with the oscillation in the PBE correlation potential near $r = 60$ leading to a large peak and valley in the energy density. However, when we look at the net area under the curve, $E_C + T_C$, we find that LSD is too negative, LYP is not negative enough, and PBE yields the closest answer to the exact one.

Hypercorrelated Potential

We have used the adiabatic connection formula [35] for the exchange–correlation energy to define a ''hypercorrelated'' potential [36], whose virial yields the exact correlation energy. This adiabatic connection relates the physical and Kohn–Sham systems in a continuous fashion, through the adiabatic coupling constant λ. We imagine multiplying the interelectronic repulsion by λ, and then varying the external potential with λ in such a way as to keep $\rho(\mathbf{r})$ fixed. At $\lambda = 0$, the wave function of our system is the noninteracting Kohn–Sham wave function and the external potential is simply the Kohn–Sham potential. At $\lambda = 1$, we recover the fully interacting physical system. As $\lambda \to \infty$, the Coulomb repulsion dominates over the kinetic energy, and the correlation becomes completely static.

The hypercorrelated potential is constructed as

$$\tilde{v}_C(\mathbf{r}) = \int_1^\infty \frac{d\lambda}{\lambda^3} v_C^\lambda(\mathbf{r}), \tag{20}$$

where

$$v_C^\lambda(\mathbf{r}) = \delta E_C^\lambda[\,\rho]/\delta\rho(\mathbf{r}), \tag{21}$$

and E_C^λ is the correlation energy at coupling constant λ [37]. For example, $E_{XC}^\lambda \approx \lambda E_X + O(\lambda^2)$ for finite systems, and $E_{XC}^{\lambda=1} = E_{XC}$. For small λ, $E_X^\lambda \sim O(\lambda)$, $E_C^\lambda \sim O(\lambda^2)$, and $E_C^\lambda + T_C^\lambda \sim O(\lambda^3)$. In Figure 6, we plot v_C^λ within the PBE approximation for values of λ between 1 and 2. At $\lambda = 1$, this is just $v_C(\mathbf{r})$, while as $\lambda \to \infty$, it grows as $\lambda^{3/2}$. Note that this growth is weaker in the low-density case, where correlation is more static.

They hypercorrelated potential of Eq. (20) is defined so that

$$-\int d\mathbf{r}\, \rho(\mathbf{r})\mathbf{r}\cdot\nabla\tilde{v}_C(\mathbf{r}) = E_C, \tag{22}$$

i.e., the correlation energy is the virial of the hypercorrelated potential. We write

$$e_C(\mathbf{r}) = -\rho(\mathbf{r})\mathbf{r}\cdot\nabla\tilde{v}_C(\mathbf{r}). \tag{23}$$

In Figure 7, we plot the hypercorrelated potentials. Note that there are no exact curves in this plot because these would require knowledge of the exact correlation potential at coupling constants other than $\lambda = 1$. In principle, it is possible to calculate the hypercorrelated potential exactly for small systems, by varying the coupling constant in an accurate wave function calculation, and choosing the external potential so as to reproduce the physical density. In practice, such a procedure would be quite computationally demanding with current techniques. Here, we calculate $\tilde{v}_C(\mathbf{r})$ only approximately, using LSD and several GGAs.

However, one can easily imagine what the exact curves might look like. Compare the curves in the left panels of Figures 3 and 7, for any given approximation. The effect of hypercorrelating the potential as in Eq. (20) is to produce a potential which is more correlated than the regular correlation potential. The two sets of curves are qualitatively similar, but the features are more pronounced in the hypercorrelated one. Thus the exact hypercorrelated curve will probably be positive at $r = 0$, but with a great value, dip down more deeply to negative values near $r = 2$, and approach 0 from above.

Repeating this procedure for the low-density system, note that the hypercorrelated potentials are much closer to their corresponding correlation potentials. This is because at low densities, most of the correlation is pure potential and little kinetic.

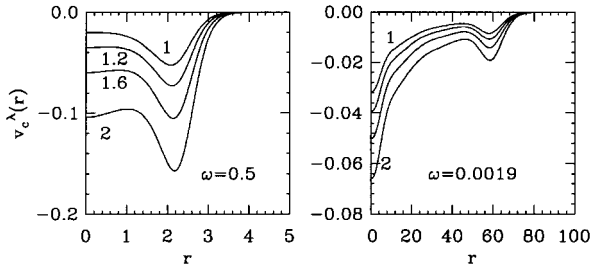

FIGURE 6. λ-dependent correlation potential in PBE for Hooke's atom.

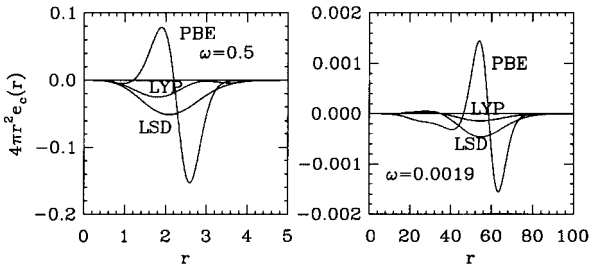

FIGURE 8. Radial virial hypercorrelated energy density in Hooke's atom.

Under these conditions, the change in potential with coupling constant is almost linear, which would make $\tilde{v}_C(\mathbf{r}) \approx v_C(\mathbf{r})$, from Eq. (20).

Figure 8 contains the radial energy density of the hypercorrelated potential and shows similar effect relative to the energy density from the correlation potential of Figure 5. Note that though the distortion of the hypercorrelated energy density relative to the correlation potential's energy density destroys some of the very precise cancellation between peak areas (in the case of the GGAs) leading to a net area equal to E_C rather than $E_C + T_C$, as would also be the case for the exact curve.

Finally, subtraction of Eq. (22) from Eq. (18) also produces a uniquely defined correlation-kinetic energy density [38],

$$T_C = \int d\mathbf{r}\, t_C(\mathbf{r}), \tag{24}$$

where

$$t_C(\mathbf{r}) = -\rho(\mathbf{r})\mathbf{r} \cdot \nabla\{v_C(\mathbf{r}) - \tilde{v}_C(\mathbf{r})\}, \tag{25}$$

which can also be compared against approximate functionals. The severe underestimation of T_C by LYP for $\omega = 0.0019$ is demonstrated by the fact that $v_C(\mathbf{r})$ and $\tilde{v}_C(\mathbf{r})$ are almost identical, leading to a far too small $t_C(\mathbf{r})$ in Eq. (25) above.

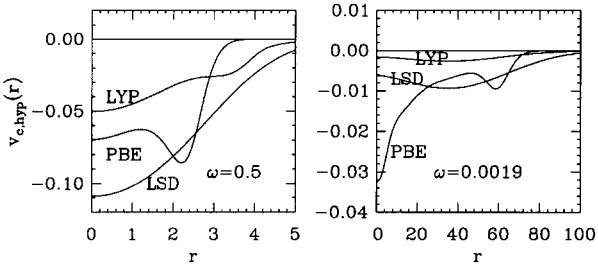

FIGURE 7. Hypercorrelated potential in Hooke's atom.

Conclusions

We have calculated the hypercorrelated potential for the Hooke's atom at both moderate and extremely low densities, within several functional approximations. The virial of this potential is the correlation energy, and so it provides a correlation energy density which is uniquely defined by the correlation energy functional.

We are currently pursuing two further applications of this work. In the first, we are attempting to construct a reliable approximation to the hypercorrelated potential, using the correlation potential itself. Such a scheme would yield a method for accurate estimation of the correlation energy, *given* the exact density [39]. In the second, we are attempting to construct the hypercorrelated potential directly from the exchange potential and the GGA approximations to both. Such a scheme would yield a nonempirical energy density hybrid at each point in space, which would admix a space-dependent amount of exchange with GGA exchange–correlation, overcoming limitations of current nonempirical schemes [9].

ACKNOWLEDGMENTS

One of us (K.B.) thanks John Perdew and Mel Levy for useful discussions. This research was supported by an award from Research Corporation.

References

1. W. Kohn and L. J. Sham, Phys. Rev. **140**, A 1133 (1965).
2. K. Burke, J. P. Perdew, and M. Levy, in *Modern Density Functional Theory: A Tool for Chemistry*, J. M. Seminario and P. Politzer, Eds. (Elsevier, Amsterdam, 1995).

3. J. P. Perdew and Y. Wang, Phys. Rev. B **33**, 8800 (1986); **40**, 3399 (1989) (E).
4. J. P. Perdew, in *Electronic Structure of Solids* '91, P. Ziesche and H. Eschrig, Eds. (Akademie, Berlin, 1991), p. 11.
5. J. P. Perdew, J. A. Chevary, S. H. Vosko, K. A. Jackson, M. R. Pederson, D. J. Singh, and C. Fiolhais, Phys. Rev. B **46**, 6671 (1992); **48**, 4978 (1993) (E).
6. J. P. Perdew, K. Burke, and Y. Wang, Phys. Rev. B **54**, 16533 (1996).
7. J. P. Perdew, K. Burke, and M. Ernzerhof, Phys. Rev. Lett. **77**, 3865 (1996); **78**, 1396 (1997) (E).
8. A. D. Becke, J. Chem. Phys. **98**, 5648 (1993).
9. K. Burke, M. Ernzerhof, and J. P. Perdew, Chem. Phys. Lett. **265**, 115 (1997).
10. M. Ernzerhof, Chem. Phys. Lett. **263**, 499 (1996).
11. S. Kais, D. R. Herschbach, N. C. Handy, C. W. Murray, and G. J. Laming, J. Chem. Phys. **99**, 417 (1993).
12. M. Taut, J. Phys. A **27**, 1045 (1994).
13. A. Zupan, K. Burke, M. Ernzerhof, and J. P. Perdew, J. Chem. Phys., **106**, 10184 (1997).
14. C. Filippi, C. J. Umrigar, and M. Taut, J. Chem. Phys. **100**, 1290 (1994).
15. J. Chen and M. J. Stott, Phys. Rev. A **44**, 2816 (1991).
16. Q. Zhao and R. G. Parr, Phys. Rev. A **46**, 2337 (1992).
17. A. Görling, Phys. Rev. A **46**, 3753 (1992).
18. Á. Nagy, J. Phys. B **26**, 43 (1993).
19. Y. Wang and R. G. Parr, Phys. Rev. A **47**, R1591 (1993).
20. C. J. Umrigar and X. Gonze, in *High Performance Computing and Its Application to the Physical Sciences*, Proceedings of the Mardi Gras 1993 Conference, D. A. Browne, et al., Eds. (World Scientific, Singapore, 1993).
21. E. V. Ludenã, R. Lopez-Boada, J. Maldonado, T. Koga, and E. S. Kryachko, Phys. Rev. A **48**, 1937 (1993).
22. R. van Leeuwen and E. J. Baerends, Phys. Rev. A **49**, 2421 (1994).
23. C. Filippi, C. Umrigar, and X. Gonze, Phys. Rev. A **54**, 4810 (1996).
24. M. Levy and J. P. Perdew, Phys. Rev. A **32**, 2010 (1985).
25. A. Görling and M. Levy, Phys. Rev. B **47**, 13105 (1993).
26. J. P. Perdew and Y. Wang, Phys. Rev. B **46**, 12947 (1992).
27. A. D. Becke, Phys. Rev. A **38**, 3098 (1988).
28. C. Lee, W. Yang, and R. G. Parr, Phys. Rev. B **37**, 785 (1988).
29. C. Filippi, X. Gonze, and C. J. Umrigar, in *Recent Developments and Applications of Modern Density Functional Theory*, J. Seminario, Ed. (Elsevier, Amsterdam, 1996).
30. K. Burke, J. P. Perdew, and M. Ernzerhof, Int. J. Quant. Chem. **61**, 287 (1997).
31. P. Süle, O. V. Grisenko, A. Nagy, and E. J. Baerends, J. Chem. Phys. **103**, 10085 (1995).
32. C. J. Huang and C. J. Umrigar, Phys. Rev. A **56**, 290 (1997).
33. K. Burke, J. P. Perdew, and Y. Wang, in *Electronic Density Functional Theory: Recent Progress and New Directions*, J. F. Dobson, G. Vignale, and M. P. Das, Eds. (Plenum, New York, 1998), p. 81.
34. E. Engel and S. H. Vosko, Phys. Rev. B **47**, 13164 (1993).
35. D. C. Langreth and J. P. Perdew, Solid State Commun. **17**, 1425 (1975).
36. K. Burke, F. Cruz, and K. C. Lam, J. Phys. Chem. A, to appear.
37. K. Burke, in *Electronic Density Functional Theory: Recent Progress and New Directions*, J. F. Dobson, G. Vignale, and M. P. Das, Eds. (Plenum, New York, 1997).
38. P. Süle, Chem. Phys. Lett. **259**, 69 (1996).
39. R. G. Parr and S. K. Ghosh, Phys. Rev. A **51**, 3564 (1995).